

Surface Reactions of Carbon Dioxide at the Adsorbed Water–Iron Oxide Interface

Jonas Baltrusaitis and Vicki H. Grassian*

Department of Chemistry, University of Iowa, Iowa City, Iowa 52242

Received: April 11, 2005

Despite the fact that carbon dioxide is an abundant atmospheric gas with profound environmental implications, there is little information on the reaction of carbon dioxide at the adsorbed water–oxide interface. In this study, the chemistry of carbon dioxide at the adsorbed water–iron oxide interface is investigated with FTIR spectroscopy. As shown here, the thin water layer on the iron oxide surface plays an important role in the surface chemistry of carbon dioxide. In particular, adsorbed water enhances CO₂ uptake, undergoes isotope exchange with CO₂ in O(18)-labeled experiments, and influences the chemical nature of the predominant adsorbed product on the surface from bicarbonate to carbonate. The resultant thin water film is acidic in nature from the reaction of CO₂. The IR spectrum recorded of adsorbed carbonate at the adsorbed water–iron oxide interface is remarkably similar to that at the bulk liquid water–iron oxide interface. Since reactions in thin water films estimated to be ~2 layers will play a role in a number of environmental processes, it is essential to understand the chemistry of these “wet” interfaces with atmospheric gases.

Introduction

Oxide surfaces are important environmental interfaces.^{1–4} As environmental interfaces, understanding the molecular-level details of the chemistry at the adsorbed water–oxide interface is imperative if environmental chemical processes are to be fully understood.⁵ Iron oxides are common reactive components of air, water, and soil, and the surface chemistry of iron oxides under ambient conditions plays a crucial role in a number of environmental processes. For example, Fe-containing minerals such as hematite, α -Fe₂O₃, present in the atmosphere as a component of the mineral dust aerosol, are an important nutrient source for ocean life.⁶ Since the bioavailability of the iron depends on the iron oxidation state, only a fraction of the iron can be used by phytoplankton and other organisms.⁷ Recently, the surface chemistry of Fe-containing mineral dust aerosol with pollutant gases has been implicated as an important mechanism for increasing the amount of bioavailable iron through the reduction of Fe(III) to Fe(II).⁷ This process is proposed to occur in a thin aqueous layer coating the Fe-containing mineral. Thus, as an environmental interface, this thin water film will play a role in the chemistry of molecules adsorbed on iron oxide surfaces.⁸

As a first step in understanding the molecular-level details of the chemistry of the adsorbed water–iron oxide interface, we have investigated the surface chemistry of CO₂ on Fe₂O₃ nanoparticles (~30 nm in diameter) under ambient conditions of temperature and relative humidity. Iron oxide nanoparticles were used for several reasons, including the following: (i) The high surface area of these particles is extremely useful for spectroscopic studies, and more importantly, (ii) iron oxides commonly occur in nature as nanoparticles.⁹

Although iron oxide interfaces have been studied under vacuum conditions and in contact with bulk aqueous solutions, to our knowledge, this is the first reported study to investigate

the surface chemistry of CO₂ at the adsorbed water–iron oxide interface. Not including H₂O vapor, CO₂ is the fourth most abundant gas in the atmosphere after N₂, O₂, and Ar.¹⁰ As the most abundant greenhouse gas, its sources, sinks, and chemistry must be understood.¹¹ As shown here, the thin water layer on the surface of the Fe₂O₃ particle plays an important role in the surface chemistry of CO₂. In particular, adsorbed water enhances CO₂ uptake, undergoes isotope exchange with CO₂ in O(18) labeled experiments, and influences the chemical nature of the predominant adsorbed product on the surface from bicarbonate to carbonate. In addition, reaction of CO₂ at the adsorbed water–oxide interface results in an acidic water layer.

Experimental Section

Two types of FTIR experiments were employed in this study. The first involves transmission IR spectroscopy of iron oxide in the presence of gas-phase CO₂.^{12,13} The experimental apparatus used in these measurements has been described in detail before. A tungsten grid placed between nickel jaws is half-coated with iron oxide nanoparticles, and the other half of the grid is left blank. The nickel jaw with the half-coated tungsten grid is placed inside a stainless steel cube which has two BaF₂ windows. The cube is attached to a vacuum/gas handling system that can be evacuated with a turbomolecular pump. The cube sits on a linear translator inside the internal compartment of the FTIR spectrometer. This experimental setup allows for the IR spectrum to be recorded from either the half of the grid coated with iron oxide nanoparticles or the other half that is blank. Thus, the spectrum of the gas phase alone or the spectrum of surface-adsorbed molecules plus the gas phase can be recorded under identical conditions of CO₂ pressure and relative humidity.

Attenuated total reflection (ATR)-FTIR spectroscopy is also used in these studies. ATR-FTIR spectroscopy is a powerful tool for studying surface adsorption from aqueous solutions.¹⁴

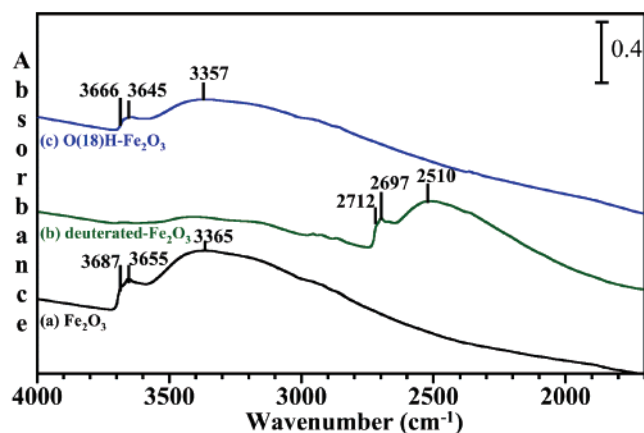


Figure 1. (a) O–H stretching region for unlabeled hydroxylated Fe_2O_3 . (b) Shift in absorption bands following isotope exchange with D_2O to give a predominantly O–D terminated surface denoted as deuterated- Fe_2O_3 . (c) Shift in absorption bands following isotope exchange with $\text{H}_2\text{O}(18)$ to give a predominantly O(18)–H terminated surface denoted as O(18)H- Fe_2O_3 .

A horizontal ATR cell purchased from Pike Technologies was used to investigate adsorption from solution onto Fe_2O_3 nanoparticles. A thin layer of Fe_2O_3 nanoparticles was prepared by making a hydrosol of the Fe_2O_3 powder and then allowing the water to evaporate. This process leaves behind a thin layer of Fe_2O_3 that uniformly coats and adheres well to the ZnSe element. The entire horizontal ATR cell is placed inside the internal compartment of the FTIR spectrometer that contains optics for the ATR cell (Pike Technologies). Pure water or solutions containing bicarbonate are then introduced into the ATR cell, and IR spectra are recorded. Solution phase spectra alone can also be recorded in the absence of the thin Fe_2O_3 -layer film. All IR spectra (ATR and transmission) were recorded at 295 K.

The iron oxide nanoparticles used in this study were purchased from Alfa Aesar (99.95% purity). Several different water samples were used, including unlabeled water purchased from Fisher Scientific (Optima grade), deuterium labeled water, D_2O , purchased from Aldrich (99.9 atom % D), and O(18) labeled water, $\text{H}_2\text{O}(18)$, purchased from ISOTEC (minimum purity 97 atom % O(18)). Carbon dioxide was purchased from Air Products.

Results and Discussion

In these studies, several isotope experiments were done to gain a better understanding of the reaction chemistry of CO_2 on Fe_2O_3 nanoparticles in the presence and absence of an adsorbed water layer. The IR spectrum of unlabeled Fe_2O_3 nanoparticles following evacuation of the IR cell to $\sim 1 \times 10^{-5}$ Torr overnight is shown in Figure 1. Absorption bands observed at 3687, 3655, and 3365 cm^{-1} are due to isolated and hydrogen-bonded O–H groups on the surface along with a small amount of adsorbed water.^{15,16} Under these dry conditions, the iron oxide particle surface is fully hydroxylated with a minimal amount of molecularly adsorbed water (<0.01 ML).¹⁷ The surface hydroxyl groups can be exchanged by reaction of Fe_2O_3 with either D_2O or $\text{H}_2\text{O}(18)$ at 10–20 Torr water vapor pressure for several hours at 295 K and 373 K, respectively. The exchange was followed by monitoring the loss of the absorption bands associated with the unlabeled O–H groups concomitant with the growth of the labeled hydroxyl group absorptions. Following the completion of the exchange reaction, the surfaces are terminated by either O–D or O(18)–H groups. The IR spectrum following deuterium

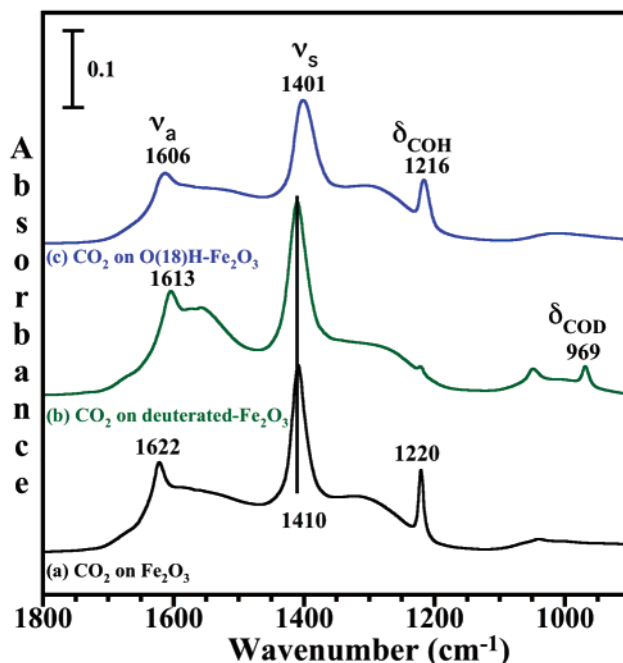
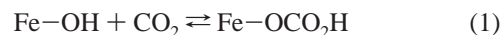


Figure 2. FTIR spectra are shown for Fe_2O_3 in the presence of gas-phase CO_2 at a pressure of 275 mTorr for (a) $\text{CO}_2(16)$ adsorbed on Fe_2O_3 , (b) $\text{CO}_2(16)$ adsorbed on deuterated Fe_2O_3 , and (c) $\text{CO}_2(16)$ adsorbed on O(18) labeled Fe_2O_3 . Gas-phase absorptions have been subtracted from the spectra. The main absorptions labeled in the spectra can be assigned to adsorbed bicarbonate. See text for further details.

exchange is shown in Figure 1b and labeled “deuterated- Fe_2O_3 ”. Absorption bands associated with O–D groups on the surface are seen at 2712, 2697, and 2510 cm^{-1} . The IR spectrum recorded following surface reaction with $\text{H}_2\text{O}(18)$ is shown in Figure 1c. Absorption bands are shifted from the unlabeled surface to 3666, 3645, and 3357 cm^{-1} for the O(18)H- Fe_2O_3 surface.

The IR spectra recorded of the unlabeled and labeled Fe_2O_3 nanoparticles under dry conditions in the presence of CO_2 , at atmospherically relevant pressures, are shown in Figure 2. On the basis of spectral assignments made in the literature^{17,18} and the frequency observed for the three isotope experiments, the three main absorption bands in the spectra can be readily assigned to the formation of bicarbonate on the surface according to reaction 1



The three main absorptions can be assigned to the ν_a , ν_s , and δ_{COH} vibrations of adsorbed bicarbonate, as indicated in Figure 2. For the unlabeled surface, these peaks are at 1622, 1410, and 1220 cm^{-1} , respectively. As expected, there are some small shifts in the ν_a and ν_s for the isotope labeled surfaces, and a large shift is seen for the bending mode in the case of deuterated Fe_2O_3 . In this case, the δ_{COD} band shifts to 969 from 1220 cm^{-1} . In addition to absorptions due to bicarbonate, there is also evidence for some carbonate on the surface as indicated by the broad absorptions on the low and high cm^{-1} sides of the bicarbonate symmetric stretch along with a band near 1050 cm^{-1} (vide infra).

Similar studies of CO_2 adsorption on Fe_2O_3 were done at higher relative humidity, in the presence of water vapor. Before showing the spectra obtained in these experiments, the ATR-FTIR spectrum of carbonate adsorbed on Fe_2O_3 nanoparticles from an aqueous bicarbonate solution is shown in Figure 3a. The reason for showing this spectrum first becomes readily

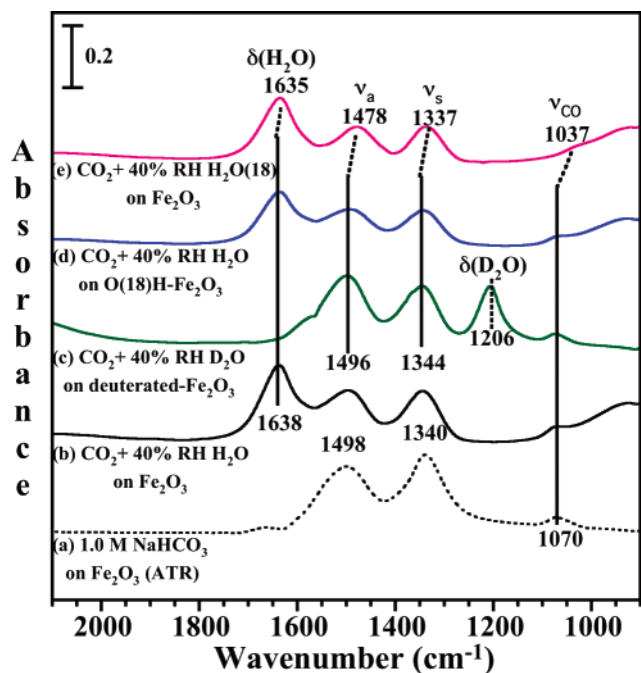


Figure 3. FTIR spectra are shown for Fe_2O_3 in the presence of (a) 1 M NaHCO_3 solution at pH = 8; solution-phase absorptions have been subtracted from the ATR spectrum. The other spectra (b)–(e) are in the presence of gas-phase CO_2 (16) at a pressure of 275 mTorr and 40% RH: (b) H_2O (16) on Fe_2O_3 , (c) D_2O on deuterated- Fe_2O_3 , (d) H_2O (16) on O(18) labeled Fe_2O_3 , and (e) H_2O (18) on O(16) labeled Fe_2O_3 . Gas-phase absorptions have been subtracted from the transmission spectra shown in (b)–(e). The absorptions labeled in the spectra are assigned to adsorbed carbonate and adsorbed water. See text for further details.

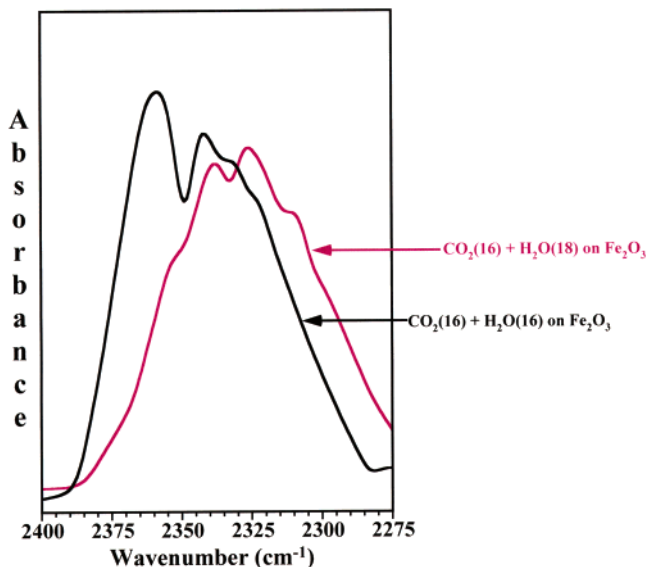
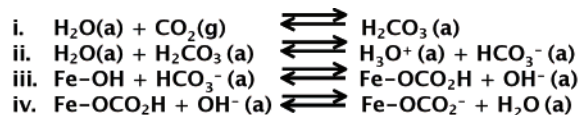


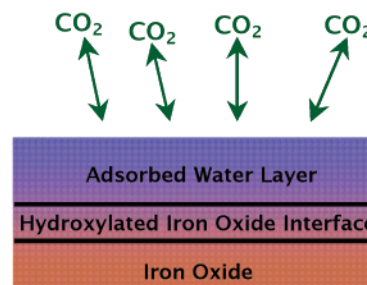
Figure 4. Gas-phase carbon dioxide following reaction of CO_2 (16) in the presence of H_2O (16) (black) on Fe_2O_3 and H_2O (18) (pink) on Fe_2O_3 . The data show that there is some shift in the absorption band in the presence of the O(18) label water because of the formation of CO -(16)O(18). These gas-phase IR spectra correspond to the IR spectra recorded for adsorbed species shown in Figure 3 (spectra labeled b and e).

apparent when comparing it to the IR spectrum recorded in the presence of water vapor corresponding to 40% relative humidity (RH) and a CO_2 pressure of 275 mTorr (Figure 3b). It can be seen that the solution-phase iron oxide spectrum and the spectrum recorded at the adsorbed water–iron oxide interface are remarkably similar given that at 40% RH the water film is

SCHEME 1: Surface Reactions of CO_2 and H_2O on Fe_2O_3



Net Rx:



estimated to be around 2 ML.¹⁹ The absorptions at 1496, 1344, and 1070 cm^{-1} in the spectrum shown in Figure 3b are assigned to the vibrational modes of the adsorbed carbonate most likely in a monodentate bonding configuration.^{17,18} These modes are labeled as ν_a , ν_s , and ν_{CO} , respectively. The spectra recorded in the presence of 40% RH D_2O (Figure 3c) are identical except for the shift in the bending mode of adsorbed water from 1638 to 1206 cm^{-1} and therefore consistent with the assignment of the carbonate spectrum.

Two additional labeling experiments using O(18) were done in an effort to better understand the surface chemistry of CO_2 at the adsorbed water–iron oxide interface. In the first experiment, H_2O (16) was coadsorbed with CO_2 (16) on an Fe–O(18)H surface, and in the second experiment, H_2O (18) was coadsorbed with CO_2 (16) on an Fe–O(16)H surface. It can be seen that there is a negligible shift in the carbonate absorption bands in the experiment using FeO(18)H and H_2O (16) in Figure 3d. However, when the O(18) label is in the water molecules, there are shifts in the vibrational modes of adsorbed carbonate indicating that the oxygen atom in H_2O (18) ends up in the carbonate product. In addition, in the H_2O (18) labeled experiments, O(18) ends up in the gas-phase CO_2 present in these experiments. Figure 4 shows the spectra recorded of the gas in equilibrium with the spectra shown in Figure 3 (spectra labeled b and d). There is a shift in absorption bands due to the formation of CO (16)O(18).

One mechanism that can explain the observed results is shown in Scheme 1. It involves the direct reaction of H_2O and CO_2 to yield carbonic acid, which deprotonates into bicarbonate. Bicarbonate then goes on to displace OH on the surface, followed by deprotonation of adsorbed bicarbonate. The last two steps in this mechanism are taken from the solution-phase mechanism proposed by Su and Suarez.¹⁸ Evidence for this mechanism includes the work of Henderson who showed that a reaction between coadsorbed CO_2 and H_2O does occur on single-crystal TiO_2 (110) at 110 K in the presence of oxygen vacancies.²⁰ Unlike the TiO_2 (110) low-temperature reaction, we determined that on Fe_2O_3 nanoparticles carbonate also forms whether water is coadsorbed simultaneously with CO_2 or adsorbed first. This mechanism explains the vibrational shifts observed in Figures 3 and 4.

In addition to the spectroscopic data shown in the H_2O (16) equilibrated gas phase, we have determined from quantitative

analysis of gas-phase CO₂ that considerably more CO₂ is adsorbed in the presence of adsorbed water. At 40% RH, it is determined that the coverage of adsorbed CO₂ on the surface increases by a factor of 5 compared to dry conditions. Thus, adsorbed water enhances the adsorption of CO₂ on iron oxide. Studies of CO₂ on NaX and γ -Al₂O₃ have similarly reported enhancement in the adsorption of CO₂ in the presence of small amounts of adsorbed water.²¹

Conclusions

The chemistry of iron oxide interfaces under ambient conditions of temperature and relative humidity plays an important role in several far-ranging processes from electrochemistry and corrosion science to environmental remediation and the atmospheric chemistry of iron-containing mineral aerosol. The thin adsorbed water layer on the iron oxide surface provides a medium for reaction and appears to become acidified in the presence of CO₂. This may influence subsequent reaction chemistry of the water layer with other gases. Further studies to understand the surface chemistry of CO₂ on iron oxides under atmospherically relevant conditions are underway along with studies of the adsorbed water–iron oxide interface with other atmospheric gases.

Acknowledgment. The authors gratefully acknowledge support from the National Science Foundation through a creativity extension of grant CHE-9984344.

References and Notes

- (1) Brown, G. E., Jr.; Henrich, V. E.; Case, W. H.; Clark, D. L.; Eggleston, C.; Felmy, A.; Goodman, D. W.; Gratzel, M.; Maciel, G.; McCarthy, M. I.; Neelson, K. H.; Sverjensky, D. A.; Toney, M. F.; Zachara, J. M. *Chem. Rev.* **1999**, *99*, 77.
- (2) Stumm, W. *Chemistry of the Solid-Water Interface*; Wiley: New York, 1992.
- (3) Al-Abadleh, H. A.; Grassian, V. H. *Surf. Sci. Rep.* **2003**, *52*, 63.
- (4) Finlayson-Pitts, B. J.; Wingen, L. M.; Sumner, A. S. D.; Ramazan, K. A. *Phys. Chem. Chem. Phys.* **2003**, *5*, 223.
- (5) Brown, G. E. *Science* **2001**, *294*, 5540.
- (6) Martin, J. H.; Fitzwater, S. E. *Nature (London)* **1988**, *331*, 341.
- (7) Zhu, X. R.; Prospero, J. M.; Millero, F. J. *J. Geophys. Res.* **1997**, *102*, 21297.
- (8) Meskhidze, N.; Chameides, W. L.; Nenes, A.; Chen, G. *Geophys. Res. Lett.* **2003**, *30* (21), 2085.
- (9) Banfield, J. F.; Zhang, H. In *Nanoparticles and the Environment*; Banfield, J. F., Navrotsky, A., Eds.; Reviews in Mineralogy and Geochemistry series 44; Mineralogical Society of America: Washington, DC, 2001; p 1.
- (10) Robbins, L. L.; Fabry, V. J. In *Carbon Dioxide Chemistry: Environmental Issues*; Paul, J., Pradier, C., Eds.; The Royal Society of Chemistry: Cambridge, U.K., 1994; pp 301–304.
- (11) Sundquist, E. T. In *The Carbon Cycle and Atmospheric CO₂: Natural Variations Archean to Present*; Sundquist, E. T., Broecker, W. S., Eds.; Geophysical Monograph 32; AGU: Washington, DC, 1985; pp 5–59.
- (12) Miller, T. M.; Grassian, V. H. *J. Am. Chem. Soc.* **1995**, *117*, 10969.
- (13) Driessen, M. D.; Goodman, A. L.; Miller, T. M.; Zaharias, G. A.; Grassian, V. H. *J. Phys. Chem. B* **1998**, *102*, 549–556.
- (14) McQuillan, A. J. *Adv. Mater.* **2001**, *13*, 1034.
- (15) Rochester, C. H.; Topham, S. A. *J. Chem. Soc., Faraday Trans.* **1979**, *75*, 1073.
- (16) Ishikawa, T.; Cai, W. Y.; Kandori, K. *Langmuir* **1993**, *9*, 1125.
- (17) Busca, G.; Lorenzelli, V. *Mater. Chem.* **1982**, *7*, 89.
- (18) Su, C.; Suarez, D. L. *Clays Clay Miner.* **1997**, *45*, 814.
- (19) Goodman, A. L.; Bernard, E. B.; Grassian, V. H. *J. Phys. Chem. A* **2001**, *105*, 6443.
- (20) Henderson, M. A. *Surf. Sci.* **1998**, *400*, 203.
- (21) Rege, S. U.; Yang, R. T. *Chem. Eng. Sci.* **2001**, *56*, 3781.